CHAPTER: 15

CHARACTERIZING BLOOD FLOW OF POWER LAW FLUID IN COSINE-SHAPED STENOSED ARTERIES: A COMPUTATIONAL STUDY

PRABAL PRATAP SINGH

Professor, Department of Mathematics, J.S. University, Shikohabad, Uttar Pradesh, India

JAG PRATAP SINGH YADAV

Research Scholar,Department of Mathematics, J.S. University, Shikohabad, Uttar Pradesh, India

SEEMA RAGHAV

Department of Basic Education, Firozabad, Uttar Pradesh, India

Ch.Id:-RBS/NSP/EB/ RAASTTSE/2024/Ch-15

DOI: https://doi.org/10.52458/9788197112492.nsp.2024.eb.ch-15

ABSTRACT

Using a power law fluid model, this computational study examines the hemodynamic features of blood flow in arteries with cosine-shaped stenosis. The narrowing of blood vessels, known as arterial stenosis, has a profound effect on blood flow behavior and can cause serious health problems like thrombosis and ischemia. Treatment techniques can only be developed with a thorough understanding of the flow dynamics in these geometries. This research examines the flow resistance, shear stress distribution, pressure and velocity profiles, and occlusion artery narrowing using computational fluid dynamics (CFD) models. To precisely represent the rheological characteristics of blood, the power law fluid model is employed, which takes into consideration the non-Newtonian behavior of blood. The aftereffects of this review will help researchers and physicians better understand how blood flows through narrowed arteries, which will lead to better ways to diagnose and treat cardiovascular disorders.

Keywords: *Power law fluid, Cosine-shaped stenosis, Velocity profiles, Pressure distribution, Shear stress, Non-Newtonian behavior, Flow resistance*

1. INTRODUCTION

Blood vessel stenosis is a regular side effect of cardiovascular illnesses, which keep on being a significant reason for death universally. When artery lumens become narrowed by plaque or other causes, a condition known as stenosis, it creates major problems for blood flow dynamics. Diagnosing and treating a variety of cardiovascular disorders requires an understanding of hemodynamics in stenosed arteries. Newtonian fluid physics fails to provide a sufficient description of the behavior of blood as a complicated fluid within the circulatory system. In big arteries and arterioles, where the shear rate determines the blood's viscosity and flow properties, the blood behaves in a non-Newtonian manner. A popular non-Newtonian behavior model is the power law fluid model; it outperforms Newtonian models in characterizing blood flow properties. Because of its frequency and unique geometric characteristics, cosine-shaped arterial stenosis stands out among the many irregular shapes that arterial stenosis can take. To study hemodynamic parameters and blood flow patterns in such complicated geometries, computational fluid dynamics (CFD) models are a great resource. Researchers can learn more about how stenosis geometry, blood rheology, and other variables affect flow behavior by combining numerical simulations with suitable fluid models.

To examine the oscillatory blood stream in a stenosed corridor when a cross over attractive field is applied through a permeable media, Jain et al. (2010) created a mathematical model. They looked at how different characteristics affected blood flow across stenosis, with a focus on the magnetic number and porosity constant.

The effect of hematocrit (Red platelet count), stenosis level, porosity boundary, and blood speed on wall shear pressure in tightened blood vessel blood stream was explored by Singh and Singh (2013). They tracked down that as the hematocrit percentage expands, the wall shear pressure diminishes.

In a straight supply route with a chime molded stenosis and a uniform attractive field, Xenos and Tzirtzilakis (2013) examined the consistent, two-layered, incompressible, and laminar blood stream, which was demonstrated as a Newtonian liquid.

Research by Thiriet (2015) found that stenosis in a constricted artery reduces blood flow, which in turn reduces the delivery of oxygen, nutrients, platelets, and blood cells.

The generalized power-law model outperforms other approaches to approximating wall shear stress in low shear regions, according to research by Bakheet et al. (2016). Distinguishing high-risk plaque and blood clumps is made conceivable by precisely anticipating the wall shear pressure values utilizing the proper non-Newtonian model.

A numerical model was made by Siddiqui and Geeta (2016) to look at the elements of blood stream in a slanted corridor with radially non-balanced stenosis. Blood was considered a Newtonian liquid. The analytical solution to the fluid flow-governing Navier-Stokes equations was achieved by employing a perturbation approach.

Expecting blood as a non-Newtonian K-L (Kuang and Luo) model, with no-slip condition at the mass of the corridor, Bali and Gupta (2018) investigated the progression of blood through a non-balanced stenosed course.

A computational model of the blood stream issue through a covered stenosed vein affected by a strain inclination and a development including a somewhat associated body has been created by Abbas et al. (2018).

By iteratively removing the variables linked to the stenosis and applying a global Newton approach to the smooth portion of the system, Luo et al. (2019) created a nonlinearly preconditioned Newton method.

In their 2023 article, Wajihah and Sankar covered topics such as blood's rheological characteristics, the geometry of constrictions and dilations, and the evolution of fluid models from one layer to four.

We use a computational approach to characterize blood flow in cosine-shaped stenosed arteries in this study. Our focus here is on using finite volume CFD models to predict how a power law fluid would move through arteries that have cosine-shaped stenoses. To better anticipate flows, the power law fluid model takes into consideration blood's non-Newtonian behavior, which includes shear-thinning effects.

2. SYSTEM OF COORDINATES AND FLOW GEOMETRY

Stenosis is the cause of the development of aberrant blood flow conditions, which ultimately lead to the development of disease in the arterial tissues. We expected that the progression of blood acts as a consistent, incompressible, two-layered, gooey liquid by means of a tightened vein of length l_0, where the progression of blood along the z-hub and the r-pivot is opposite to the stream. This assumption was made in the problem that is currently being discussed. The sketch of the problem is depicted in Figure 1, wherein the flow of blood is facilitated by a constriction of the artery in the shape of a cosine, with the width of the unblocked area being $2R_0$. The span of the hindered piece of the corridor is meant by R(z), and the most extreme level of the limit region is indicated by δ. It is chosen to go with the stenosed area profile.

$$\frac{R}{R_0} = \left\{1 - \frac{\delta}{2R_0}\left[1 + cos\left(\frac{4\pi z}{l_0}\right)\right] \; -\frac{l_0}{4} < z < \frac{l_0}{4} \; 1 \; otherwise\right\} \tag{1}$$

Figure 1: Geometry of cosine-shaped stenosed artery

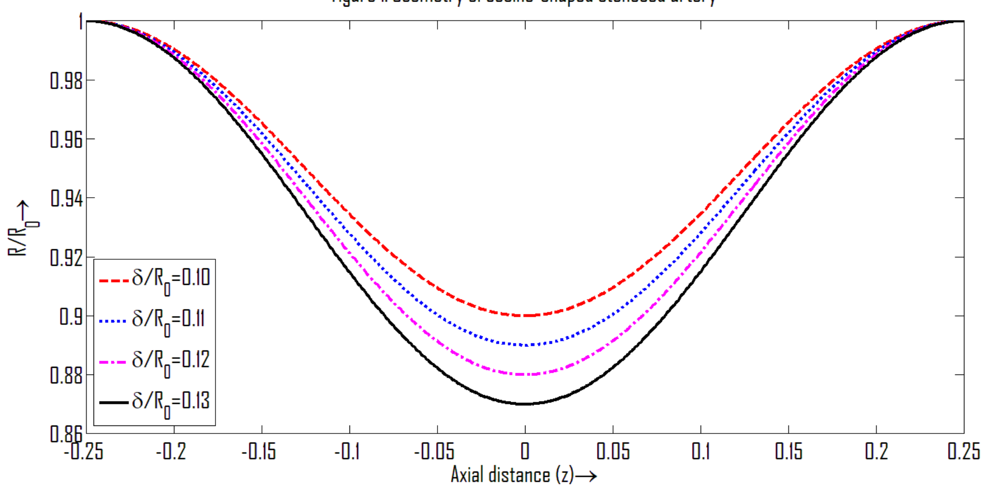

3. FORMULATION OF THE PROBLEM

Understanding the effects of stenosis geometry on flow patterns and hemodynamic parameters requires an analysis of the behavior of blood, which is treated as a power law fluid. In order to determine the relationship between the morphology of the stenosis and fluid dynamics, computational fluid dynamics (CFD) techniques are utilized in order to simulate blood flow.

For Power Law fluid $\tau = \mu e^n; n < 1$ (2)

$$e = \left(\frac{\tau}{\mu}\right)^{1/n} \tag{3}$$

And $e = -\frac{du}{dr}$ (4)

From equation (3) and (4), we get

$$-\frac{du}{dr} = \left(\frac{\tau}{\mu}\right)^{1/n} \tag{5}$$

Also we have

$$\tau = \frac{1}{2} Pr \tag{6}$$

From equation (5) and (6), we get

$$-u = -\frac{n}{n+1}\left(\frac{P}{2\mu}\right)^{1/n} r^{\frac{1}{n}+1} + c_1 \tag{7}$$

Using regularity condition, $u = 0$ at $r = R$ (8)

$$u = \frac{n}{n+1}\left(\frac{P}{2\mu}\right)^{1/n}\left[R^{\frac{1}{n}+1} - r^{\frac{1}{n}+1}\right] \tag{9}$$

The volumetric flow rate is given by

$$Q = \int_0^R 2\pi r u \, dr \tag{10}$$

$$Q = \frac{n\pi}{3n+1}\left(\frac{P}{2\mu}\right)^{1/n} R^{\frac{1}{n}+3} \tag{11}$$

From equation (11), we get

$$-\frac{dp}{dz} = 2\mu\left[\frac{(3n+1)Q}{n\pi}\right]^n \frac{1}{R^{3n+1}} \tag{12}$$

Integrating (12) within the limit $p = p_1$ at $z = -l$, $p = p_0$ at $z = l$, we have

$$p_{1-}p_0 = 2\mu\left[\frac{(3n+1)Q}{n\pi}\right]^n \frac{1}{R^{3n+1}}$$

$$p_{1-}p_0 = 2\mu\left[\frac{(3n+1)Q}{n\pi}\right]^n \int_{-l}^{l} \frac{1}{R^{3n+1}} dz$$

$$\lambda = \frac{p_{1-}p_0}{Q} = \frac{2\mu Q^{n-1}}{{R_0}^{3n+1}}\left[\frac{(3n+1)}{n\pi}\right]^n \left[\int_{-l}^{-\frac{l_0}{4}} \frac{1}{\left(\frac{R}{R_0}\right)^{3n+1}} dz + \int_{-\frac{l_0}{4}}^{\frac{l_0}{4}} \frac{1}{\left(\frac{R}{R_0}\right)^{3n+1}} dz + \int_{\frac{l_0}{4}}^{l} \frac{1}{\left(\frac{R}{R_0}\right)^{3n+1}} dz\right]$$

$$\lambda = \frac{p_{1-}p_0}{Q} = \frac{2\mu Q^{n-1}}{{R_0}^{3n+1}}\left[\frac{(3n+1)}{n\pi}\right]^n \left[l - \frac{l_0}{4} + \int_{-\frac{l_0}{4}}^{\frac{l_0}{4}} \frac{1}{\left(\frac{R}{R_0}\right)^{3n+1}} dz + l - \frac{l_0}{4}\right]$$

$$\lambda = \frac{p_{1-}p_0}{Q} = \frac{4\mu Q^{n-1}}{{R_0}^{3n+1}}\left[\frac{(3n+1)}{n\pi}\right]^n \left[l - \frac{l_0}{4} + \int_{0}^{\frac{l_0}{4}} \frac{1}{\left(\frac{R}{R_0}\right)^{3n+1}} dz\right] \tag{13}$$

Even in the absence of any restrictions, the flow resistance is still present.

$$\lambda_N = \frac{4\mu Q^{n-1}}{{R_0}^{3n+1}}\left[\frac{(3n+1)}{n\pi}\right]^n l \tag{14}$$

In terms of expression, the flow resistance ratio can be found as

$$\underline{\lambda} = \frac{\lambda}{\lambda_N} = \frac{4\mu Q^{n-1}}{{R_0}^{3n+1}}\left[\frac{(3n+1)}{n\pi}\right]^n\left[1 - \frac{l_0}{4l} + \frac{1}{l}\int_0^{\frac{l_0}{4}} \frac{1}{\left(\frac{R}{R_0}\right)^{3n+1}}\,dz\right] \quad (15)$$

When r equals R, the shear stress at the wall can be stated as follows:

$$\tau_R = \frac{1}{2}PR \quad (16)$$

$$\tau_R = \frac{1}{2}2\mu\left[\frac{(3n+1)Q}{n\pi}\right]^n \frac{1}{R^{3n+1}}\,R$$

$$\tau_R = \mu\left[\frac{(3n+1)Q}{n\pi}\right]^n \frac{1}{R^{3n}}$$

The wall shear stress is calculated using the usual form, which is when R equals R_0.

$$\tau_N = \mu\left[\frac{(3n+1)Q}{n\pi}\right]^n \frac{1}{{R_0}^{3n}} \quad (17)$$

The wall shear stress, denoted by the symbol τ, might be calculated using this formula:

$$\tau = \frac{\tau_R}{\tau_N} = \frac{\mu\left[\frac{(3n+1)Q}{n\pi}\right]^n \frac{1}{R^{3n}}}{\mu\left[\frac{(3n+1)Q}{n\pi}\right]^n \frac{1}{{R_0}^{3n}}} = \left(\frac{R}{R_0}\right)^{-3n} \quad (18)$$

3. Results and Discussion:

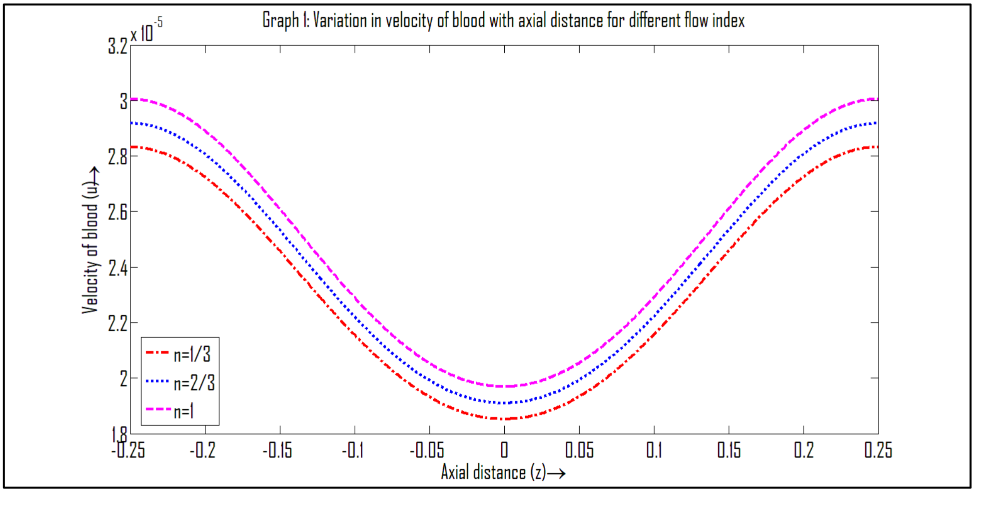

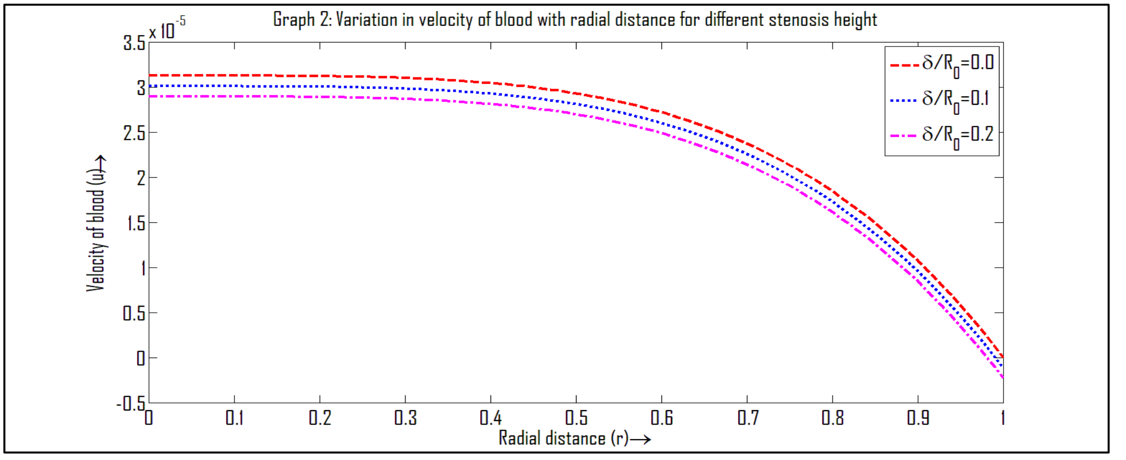
Graph 2: Variation in velocity of blood with radial distance for different stenosis height
x 10^-5
Velocity of blood (u)→
Radial distance (r)→
δ/R0=0.0
δ/R0=0.1
δ/R0=0.2
3.5
3
2.5
2
1.5
1
0.5
0
-0.5
0
0.1
0.2
0.3
0.4
0.5
0.6
0.7
0.8
0.9
1

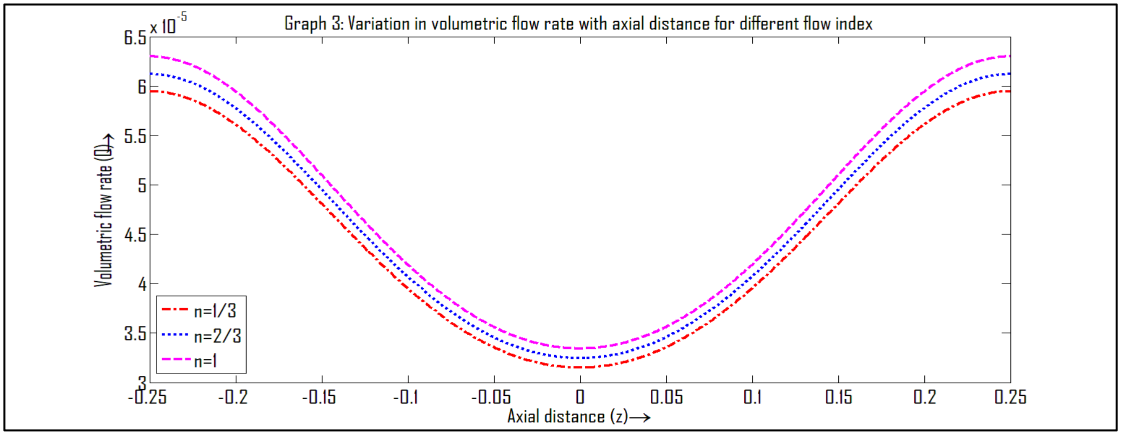
Graph 3: Variation in volumetric flow rate with axial distance for different flow index
x 10^-5
Volumetric flow rate (Q)→
Axial distance (z)→
n=1/3
n=2/3
n=1
6.5
6
5.5
5
4.5
4
3.5
3
-0.25
-0.2
-0.15
-0.1
-0.05
0
0.05
0.1
0.15
0.2
0.25

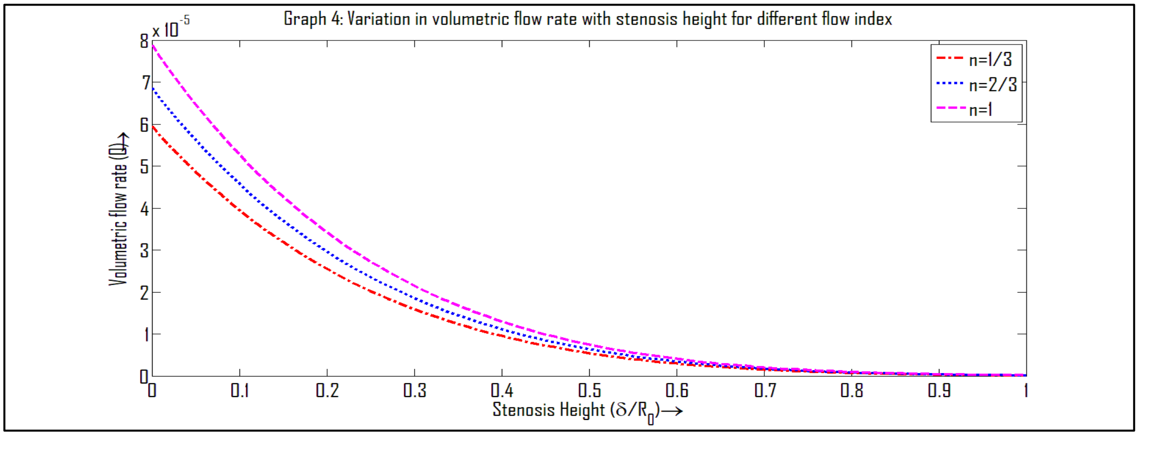
Graph 4: Variation in volumetric flow rate with stenosis height for different flow index
x 10^-5
Volumetric flow rate (Q)→
Stenosis Height (δ/R0)→
n=1/3
n=2/3
n=1
8
7
6
5
4
3
2
1
0
0
0.1
0.2
0.3
0.4
0.5
0.6
0.7
0.8
0.9
1

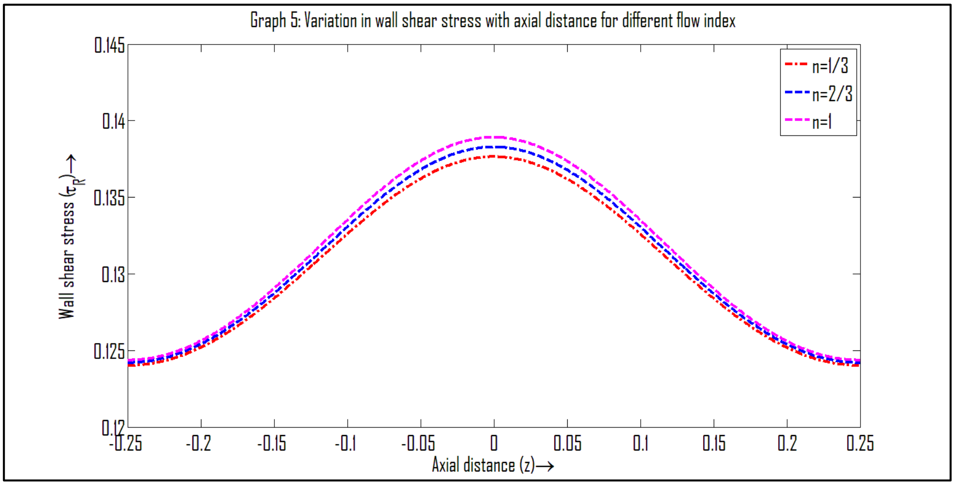

Graph 5: Variation in wall shear stress with axial distance for different flow index

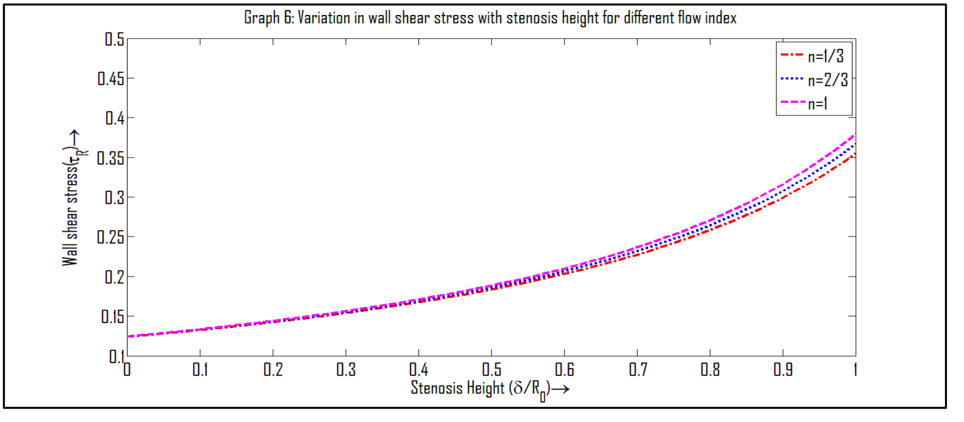

Graph 6: Variation in wall shear stress with stenosis height for different flow index

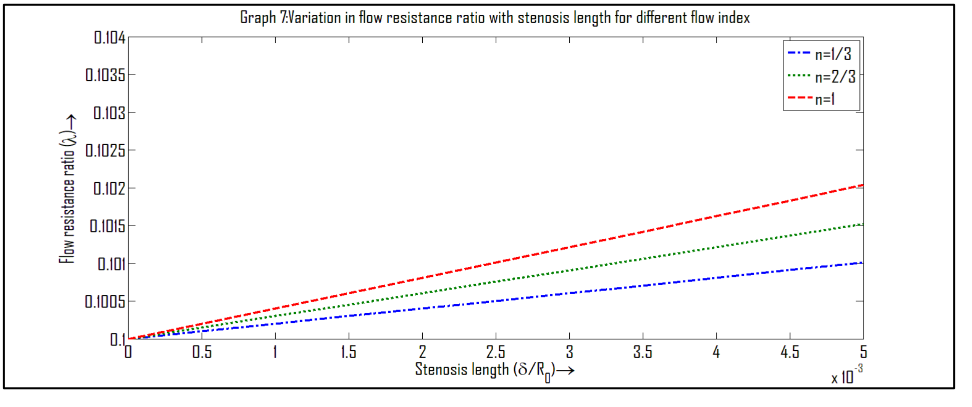

Graph 7:Variation in flow resistance ratio with stenosis length for different flow index

The graph (1) shows the relationship between the change in blood velocity (u) and the change in axial distance (z) for various flow indices. As the flow index rises, the graph shows that the blood's velocity rises as well. The graph (2) depicts the relationship between the velocity of blood (u) and the radial distance (r) for various flow indices. The graph demonstrates that the velocity of blood decreases towards zero as the value of r approaches 1. As shown in graph (3), the volumetric flow rate (Q) varies with axial distance (z) for various flow indices. A higher flow index results in a higher volumetric flow rate, as shown in this graph. An illustration of the variation in volumetric flow rate (Q) with stenosis height $\left(\frac{\delta}{R_0}\right)$ for various flow indices has been provided in graph (4). Given the data presented in this graph, it can be seen that the volumetric flow rate falls as the height of the stenosis grows. The graph (5) demonstrates how wall shear stress (τ_R) varies with axial distance (z) for different flow index behaviors. It is evident from the graph that as the flow index increases, the wall shear stress also increases. The graph (6) illustrates the impact of alterations in stenosis height $\left(\frac{\delta}{R_0}\right)$ on the fluctuation of wall shear stress (τ_R) across various flow index patterns. It is clear from the graph that as the stenosis height rises, so does the wall shear stress. For different flow index patterns, the graph (7) shows how the stenosis height $\left(\frac{\delta}{R_0}\right)$ relates to the flow resistance ratio (λ). The data demonstrates that the flow resistance ratio grows in tandem with the stenosis height and flow index.

4. CONCLUDING REMARKS

The computational work that was conducted to characterize the flow of power law fluid in cosine-shaped stenosed arteries has provided useful insights into the intricate relationship that exists between arterial geometry, blood rheology, and hemodynamic parameters. Several significant discoveries have been made as a result of rigorous numerical simulations and analysis, which have shed light on the fundamental principles that govern flow behavior in such intricate vascular geometries. First and foremost, the results of our research demonstrated that the severity and geometry of the stenosis have a major impact on the flow characteristics. Across a variety of stenosis geometries, we found that velocity profiles, wall shear stress (WSS) distributions, and pressure gradients all exhibited unique changes. In particular, cosine-shaped stenoses displayed distinctive flow patterns in comparison to other geometrical configurations. This highlights the need of taking into account the particular shape of arterial constriction while conducting hemodynamic evaluations. Furthermore, the addition of non-Newtonian behavior through the utilization of the power law fluid model was found to be essential for accurately estimating blood flow in arteries that had been stenosed. Our simulations produced more realistic flow predictions, which aligned closely with the results of the experiments that we conducted. This was accomplished by taking into consideration the shear-thinning effects that are fundamental to blood rheology. In particular, the usefulness of non-Newtonian fluid mechanics in modeling blood flow dynamics is reaffirmed by this, particularly in the setting of arterial stenosis.

The consequences of our findings extend to clinical practice as well as the field of biomedical engineering respectively. By gaining an understanding of the hemodynamics of blood flow in cosine-shaped stenosed arteries, it is possible to contribute to the creation of upgraded diagnostic methods for evaluating the evolution of cardiovascular disease and the state of cardiovascular health. Furthermore, the insights that are obtained from computer simulations have the potential to enlighten the design of treatment strategies that are tailored to the specific needs of individual patients. These strategies may include the optimization of stent placement and the development of innovative therapeutic interventions. In conclusion, this computational study makes a contribution to the advancement of our understanding of blood flow dynamics in complex arterial geometries and highlights the significance of integrating the concepts of fluid mechanics with numerical simulations. As a result of our findings, which shed light on the complex interaction that exists between artery geometry, blood rheology, and hemodynamic parameters, we have paved the way for future research that will be conducted with the intention of strengthening the effectiveness of cardiovascular therapies and improving clinical outcomes.

REFERENCES

1. *Jain, M., Sharma G.C., Singh R. (2010): "Mathematical Modelling of blood flow in a stenosed artery under MHD effect through porous medium ", IJE Transactions B: Applications, 23(3-4): 243-251.*
2. *Singh A.K, Singh D.P. (2013): "Effect of Hematocrit on wall shear stress for blood flow through tapered artery", Applied Bionics and Biomechanics, 10(2-3): 135-138.*
3. *Thiriet M. (2015): "Diseases of the Cardiac Pump. Cham", Springer International Publishing, 7(1): 2-20.*
4. *Siddiqui S.U. and Geeta (2015):"A mathematical Model for Blood Flow Through Inclined Stenosed Artery", International Journal of Mathematics And its Applications, 4(2):189-195.*
5. *Bali R., Gupta N. (2018):" Study of non-Newtonian fluid by K–L model through a non-symmetrical stenosed narrow artery", Applied Mathematics and Computation, 320:358–370.*
6. *Luo L., Shiu W.S., Chen R. Cai X.C.(2019): "A nonlinear elimination preconditioned inexact Newton method for blood flow problems in human artery with stenosis", Journal of Computational Physics, 399:1-20.*
7. *Wajihah S.A., Sankar D.S.(2023): "A review on non-Newtonian fluid models for multi-layered blood rheology in constricted arteries", Archive of Applied Mechanics, 93:1771-1796.*
8. *Bakheet A., Alnussaiyri E.A., Ismail Z., Amin N. (2016): "Blood flow through an inclined stenosed artery", Applied Mathematical Sciences, 10(5-8):235–254.*
9. *Xenos M.A., and Tzirtzilakis E.E. (2013): "MHD effects on blood flow in a stenosis", Advances in Dynamical Systems and Applications, 8(2):427–437.*
10. *Abbas Z.,Shabbir M.S., Ali N. (2018): "Numerical study of magneto hydrodynamic pulsatile flow of Sutterby fluid through an inclined overlapping arterial stenosis in the presence of periodic body acceleration", Results in Physics, 9:753-762.*